

Ionization, electron attachment, and drift in CHF₃

J. de Urquijo, I. Alvarez, and C. Cisneros

Centro de Ciencias Físicas, UNAM, P.O. Box 48-3, 62251 Cuernavaca, Morelos, México

(Received 13 April 1999)

Using a pulsed Townsend technique, we have measured the effective ionization coefficient and the electron drift velocities in CHF₃. The density-normalized electric field intensity E/N ranged from 4 to 250 townsend (Td) ($1 \text{ Td} = 10^{-17} \text{ V cm}^2$). The E/N value at which the effective ionization coefficient becomes zero was estimated to be 66 Td. For $E/N < 20$ Td, the electron attachment coefficients are practically constant, and are compatible to within about $\pm 70\%$ with previously measured values at thermal energies and above. [S1063-651X(99)08410-X]

PACS number(s): 51.50.+v, 52.25.Fi, 34.80.Lx, 34.80.Gs

Because of its importance in plasma processes related to semiconductor fabrication, trifluoromethane, or fluoroform, CHF₃ is a gas that demands basic research, since the availability of cross sections for ionization and attachment, and of electron and ion transport data is still scarce. These data are strongly needed for discharge modeling and simulation. The need for swarm and transport data on this gas has been stressed in a very recent review on the subject [1]. The only measurements on the attachment and electron drift in this gas over the density-reduced electric field strength, E/N , from 0.05 to 60 Td ($1 \text{ Td} = 10^{-17} \text{ V cm}^2$), are the recent ones of Wang *et al.* [2].

This paper reports on the measurement of the effective ionization coefficients and the electron drift velocities in CHF₃ over a wide range of E/N , from 4 to 250 Td.

The pulsed Townsend apparatus used for the present measurements has been described in detail previously [3]. Very briefly, it consists of a parallel-plate capacitor, the cathode of which is illuminated by a short flash of UV light from a 1.4 mJ nitrogen laser ($\lambda = 337 \text{ nm}$) releasing the initial photoelectrons from its surface. The highly homogeneous electric field formed between the plates causes the electrons and their ionization products to move, and these in turn produce a displacement current across the gap that is measured in the external circuit by a 40 MHz transimpedance amplifier, and registered by a 100 MHz digital oscilloscope, thereby obtaining the electron transients under the so-called “differentiated pulse condition” [4].

Vacuum base pressures in the chamber of less than 0.2 mPa were readily achieved. CHF₃ gas, with a quoted purity of 99.5% (Praxair), was admitted straight into the chamber. Gas pressures ranging between 200 Pa and 66.7 kPa were read from an absolute pressure transducer to an accuracy of 0.01% full range. All measurements were carried out at room temperatures in the range 293–300 K, measured to an accuracy of 0.2%, and gap voltage settings were estimated to be accurate to within 0.1%.

The observation of discharge development during the electron transit allows one to determine the density-normalized effective ionization coefficient $\alpha_e/N = (\alpha - \eta)/N$ and the electron drift velocity v_e , where α and η are the ionization and attachment coefficients, respectively. A typical electron component in CHF₃ is shown in Fig. 1. The

drift velocity is readily calculated from the electron transit time T_e as

$$v_e = d/T_e, \quad (1)$$

where d is gap distance. T_e is evaluated as the time elapsed between the midpoints of the rising and falling edges of the pulse, as is also shown in this figure. For a simultaneous release of n_0 photoelectrons (Dirac δ pulse), the temporal evolution of the electron current during the electron transit is given by [4]

$$I_e(t) = (n_0 q_0 / T_e) \exp(\alpha_e v_e t), \quad (2)$$

where q_0 is electron charge. A least squares fitting analysis of the exponential part of the electron component would give the effective ionization rate,

$$k_e = \alpha_e v_e, \quad (3)$$

from which α_e/N can be evaluated, with a previous determination of v_e . When the gas pressure is high, the ionic currents during the electron transit may contribute substantially—within a few percent—to the total, measurable current, as is apparent from the small aftercurrent in the

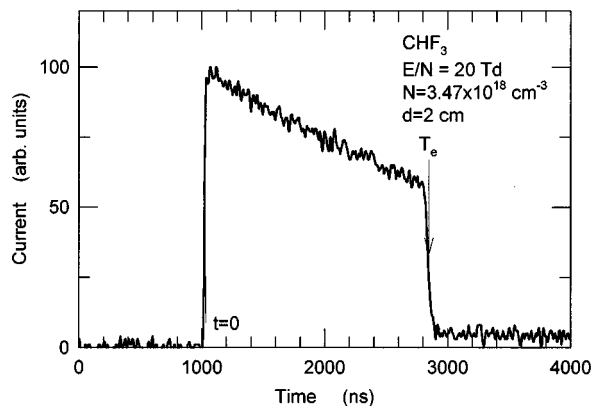


FIG. 1. A differentiated electron transient in CHF₃. The time elapsed between the marks $t=0$ and T_e indicates the electron transit time.

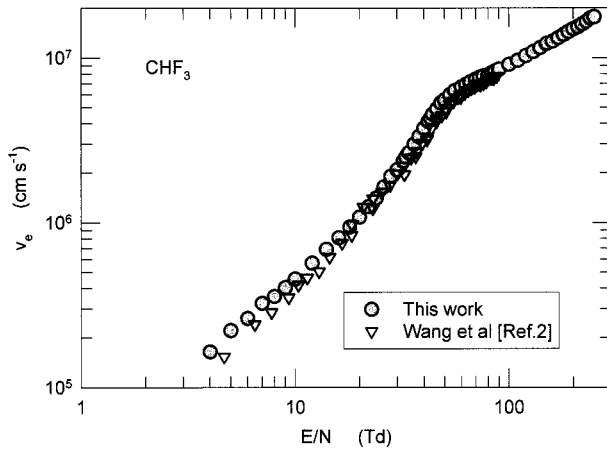


FIG. 2. The electron drift velocity in CHF_3 from this work (closed circles), and that from Ref. [2] (inverted triangles).

sample transient of Fig. 1. This contribution is readily subtracted from the total current by approximating their exponential rise to a straight line, thereby obtaining an even better measurement of the electron current only, and hence of k_e .

The electron drift velocities in CHF_3 , measured over the E/N range from 4 to 250 Td, are shown plotted in Fig. 2. Over the whole E/N range, at least two different pressures, but normally four, were used to obtain an average of v_e for each E/N value. Typical uncertainties on the v_e values are 3–4% for $E/N < 30$ Td, and 0.5–2% above.

As regards comparison with previous work, the drift velocities measured by Wang *et al.* [2] are also displayed in the same figure, and are generally lower, but normally within combined uncertainties. These authors derived their values from a pulsed Townsend experiment similar to ours, but from integrated electron transients. To the best of our knowledge, no values of v_e have been reported for $E/N > 80$ Td.

Although no electron attachment cross sections for CHF_3 have yet been reported, the review of Christophorou *et al.* [1] indicates that F^- is by far the most abundant negative ion. In connection with this, our measurements for $E/N < 60$ Td clearly indicate the presence of electron attachment processes, as is illustrated by the decaying exponential of the sample transient of Fig. 1, and predicted by Eq. (2).

Values of $\alpha_e/N = (\alpha - \eta)/N$ for $66 < E/N < 250$ Td are shown plotted in Fig. 3. Typical uncertainties over this range are 3–7%. To our knowledge, no previous values of this coefficient for $E/N > 50$ Td have been published before. The present α_e/N values have been fitted to the well-known semiempirical expression [5]

$$\frac{\alpha_e}{N} = A \exp\left(-B \frac{N}{E}\right), \quad (4)$$

with α_e/N in units of cm^2 , E/N in Td, $A = 2.6 \times 10^{-16} \text{ cm}^2$, and $B = 566 \text{ Td}^{-1}$. The overall deviation of the experimental points from the calculated ones is typically $\pm 3\%$, which is well within quoted uncertainties. The effective ionization rate coefficients k_e are also plotted in Fig. 3.

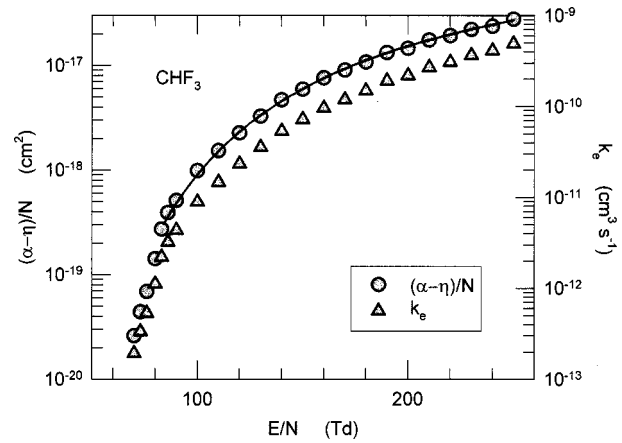


FIG. 3. The present effective ionization coefficient α_e/N in CHF_3 for $E/N > 66$ Td (circles). The solid line is the fit to the α_e/N data from Eq. (4). The effective ionization rate (triangles).

For $E/N < 66$ Td, the effective ionization coefficient becomes negative, and it decreases steadily down to about $-5 \times 10^{-19} \text{ cm}^2$ at $E/N = 4$ Td, as is shown in Fig. 4. Our measurements over this range were the result of three independent series, which produced these values consistently. Typical uncertainties range from 3% to 7% for $E/N < 30$ Td, and 10% up to $E/N = 63$ Td. This rather high uncertainty value results from the smallness of α_e/N in the region where it changes sign. We have estimated a value of $E/N_{\text{lim}} = 66$ Td, as that for which $\alpha = \eta$.

In the same figure, the effective ionization rate has been plotted, where one sees that for $E/N < 20$ Td, k_e remains essentially constant at a value of $7.9 \times 10^{-14} \text{ cm}^3 \text{ s}^{-1}$. In fact, for $E/N < 20$ Td, electron impact ionization processes in CHF_3 are either absent or negligible in comparison with electron attachment. Therefore, our effective ionization coefficients (rates) may be regarded as attachment coefficients (rates), and therefore may be compared with the thermal value of $6.2 \times 10^{-14} \text{ cm}^3 \text{ s}^{-1}$ measured by Davies, Compton, and Nelson [6], and with the value of $1.3 \times 10^{-13} \text{ cm}^3 \text{ s}^{-1}$,

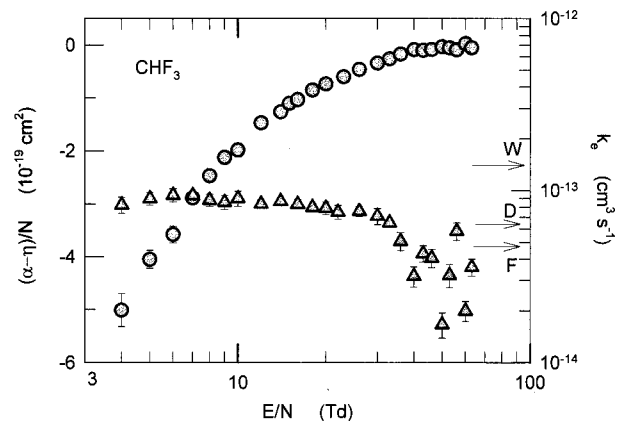


FIG. 4. The present effective ionization coefficient α_e/N in CHF_3 for $E/N < 66$ Td (circles), and the effective ionization rate k_e (triangles). The arrows on the right-hand axis are the attachment rates of (W) Wang *et al.* [2], (D) Davis, Compton, and Nelson [6], and (F) Fessenden and Bansal [7] (see text).

measured by Wang *et al.* [2] over the E/N range 1.5–50 Td. The thermal value of Fessenden and Bansal [7], also measured at thermal energies, is about 50% smaller than ours.

Further electron capture cross section measurements would shed more light on the apparently small role that this

process plays for electron energies above thermal.

This research was partially supported by DGAPA under Project No. IN113898, and by CONACYT. Thanks are due to E. Basurto and A. Bustos for their assistance.

-
- [1] L. G. Christophorou, J. K. Olthoff, and M. V. V. S. Rao, *J. Phys. Chem. Ref. Data* **26**, 1 (1997).
- [2] Yicheng Wang, L. G. Christophorou, J. K. Olthoff, and J. K. Verbrugge, in *Gaseous Dielectrics VIII*, edited by L. G. Christophorou and J. K. Olthoff (Kluwer Academic/Plenum Publishers, New York, 1999), pp. 39–43; Y. Wang, L. G. Christophorou, J. K. Olthoff, and J. K. Verbrugge, *Chem. Phys. Lett.* **304**, 303 (1999).
- [3] J. de Urquijo, C. A. Arriaga, I. Alvarez, and C. Cisneros, *J. Phys. D* **32**, 41 (1999).
- [4] H. Raether, *Electron Avalanches and Breakdown in Gases* (Butterworths, London, 1964).
- [5] E. Nasser, *Fundamentals of Gaseous Ionization and Plasma Electronics* (Wiley, New York, 1971).
- [6] F. J. Davis, R. N. Compton, and D. R. Nelson, *J. Chem. Phys.* **59**, 2324 (1973).
- [7] R. W. Fessenden and K. M. Bansal, *J. Chem. Phys.* **53**, 3468 (1970).